Dipolar-octupolar Ising antiferromagnetism in Sm_{2}Ti_{2}O_{7}: A moment fragmentation candidate

C. Mauws, A. M. Hallas, G. Sala, A. A. Aczel, P. M. Sarte, J. Gaudet, D. Ziat, J. A. Quilliam, J. A. Lussier, M. Bieringer, H. D. Zhou, A. Wildes, M. B. Stone, D. Abernathy, G. M. Luke, B. D. Gaulin, and C. R. Wiebe

Phys. Rev. B **98**, 100401 — Published 5 September 2018

DOI: 10.1103/PhysRevB.98.100401

Dipolar-Octupolar Ising Antiferromagnetism in $Sm_2Ti_2O_7$: A Moment Fragmentation Candidate

C. Mauws,[1,2] A. M. Hallas,[3,4] G. Sala,[5] A. A. Aczel,[5] P. M. Sarte,[6,7] J. Gaudet,[3] D. Ziat,[8] J. A. Quilliam,[8] J. A. Lussier,[1] M. Bieringer,[1] H. D. Zhou,[9,10] A. Wildes,[11] M. B. Stone,[5] D. Abernathy,[5] G. M. Luke,[3,12,13] B. D. Gaulin,[3,12] and C. R. Wiebe[1,2,3,12]

[1] *Department of Chemistry, University of Manitoba, Winnipeg R3T 2N2, Canada*
[2] *Department of Chemistry, University of Winnipeg, Winnipeg R3B 2E9, Canada*
[3] *Department of Physics and Astronomy, McMaster University, Hamilton L8S 4M1, Canada*
[4] *Department of Physics and Astronomy and Rice Center for Quantum Materials, Rice University, Houston, TX, 77005 USA*
[5] *Neutron Scattering Division, Oak Ridge National Laboratory, Oak Ridge, Tennessee 37831, USA*
[6] *School of Chemistry, University of Edinburgh, Edinburgh EH9 3FJ, United Kingdom*
[7] *Centre for Science at Extreme Conditions, University of Edinburgh, Edinburgh EH9 3FD, United Kingdom*
[8] *Institut Quantique and Département de Physique, Université de Sherbrooke, Sherbrooke, Québec J1K 2R1, Canada*
[9] *Department of Physics and Astronomy, University of Tennessee-Knoxville, Knoxville 37996-1220, United States*
[10] *National High Magnetic Field Laboratory, Florida State University, Tallahassee 32306-4005, United States*
[11] *Institut Laue-Langevin, 71 avenue des Martyrs, CS 20156, 38042 Grenoble Cedex 9, France*
[12] *Canadian Institute for Advanced Research, Toronto M5G 1M1, Canada*
[13] *TRIUMF, 4004 Wesbrook Mall, Vancouver, British Columbia, Canada V6T 2A3*

(Dated: August 20, 2018)

Over the past two decades, the magnetic ground states of all rare earth titanate pyrochlores have been extensively studied, with the exception of $Sm_2Ti_2O_7$. This is, in large part, due to the very high absorption cross-section of naturally-occurring samarium, which renders neutron scattering infeasible. To combat this, we have grown a large, isotopically-enriched single crystal of $Sm_2Ti_2O_7$. Using inelastic neutron scattering, we determine that the crystal field ground state for Sm^{3+} is a dipolar-octupolar doublet with Ising anisotropy. Neutron diffraction experiments reveal that $Sm_2Ti_2O_7$ orders into the all-in, all-out magnetic structure with an ordered moment of 0.44(7) μ_B below $T_N = 0.35$ K, consistent with expectations for antiferromagnetically-coupled Ising spins on the pyrochlore lattice. Zero-field muon spin relaxation measurements reveal an absence of spontaneous oscillations and persistent spin fluctuations down to 0.03 K. The combination of the dipolar-octupolar nature of the Sm^{3+} moment, the all-in, all-out ordered state, and the low-temperature persistent spin dynamics make this material an intriguing candidate for moment fragmentation physics.

Rare earth titanate pyrochlores of the form $R_2Ti_2O_7$ have long been a centerpiece in the study of geometrically-frustrated magnetism [1]. In this family of materials, the magnetism is carried by the R^{3+} rare earth ions, which decorate a network of corner-sharing tetrahedra.The study of this family has led to the discovery of a range of fascinating ground states such as the dipolar spin ice state, which was first observed in $Ho_2Ti_2O_7$ and $Dy_2Ti_2O_7$ [2–4]. Here local Ising anisotropy combines with dominant dipolar interactions, which are ferromagnetic at the nearest neighbour level on the pyrochlore lattice [5]. The spin ice state is characterized by individual tetrahedra obeying two-in, two-out "ice rules", wherein two spins point directly towards the tetrahedron's center and the other two spins point outwards (left inset of Fig. 1). This configuration can be achieved in six equivalent ways for a single tetrahedron, giving rise to a macroscopic degeneracy for the lattice as a whole. In other titanates, where the rare earth moments are smaller than in $Ho_2Ti_2O_7$ and $Dy_2Ti_2O_7$, dipolar interactions become less important and exchange interactions tend to dominate. This is exactly the case when $R = Sm^{3+}$ ($\sim 1\ \mu_B$), where the magnetic moment is reduced by a factor of ten from $R = Ho^{3+}$ and Dy^{3+} ($\sim 10\ \mu_B$), corresponding to dipolar interactions that are weaker by two orders of magnitude.

In this letter we show that anitferromagnetically coupled Ising spins with negligible dipolar interactions give rise to an all-in, all-out (AIAO) magnetic ground state in $Sm_2Ti_2O_7$. The AIAO structure is characterized by adjacent tetrahedra alternating between all spins pointing inwards and all spins pointing outwards (right inset of Fig. 1). Unlike the ferromagnetic spin ice state, the antiferromagnetic AIAO state does not give rise to a macroscopic degeneracy; placing a single spin as "in" or "out" is enough to uniquely constrain the orientations of all other spins on the lattice. A host of neodymium pyrochlores with varying non-magnetic B sites also display the AIAO ground state, $Nd_2B_2O_7$ (B = Sn, Zr, Hf) [6–9]. $Nd_2Zr_2O_7$ is a particularly interesting case as magnetic Bragg peaks from the AIAO structure and disordered, spin ice-like diffuse scattering coexist at low temperatures [10]. This exotic phenomenology has been termed moment fragmentation [11]. Recent theoretical work [12] has argued that the origin of this effect is the peculiar dipolar-octupolar symmetry of the Nd^{3+} ground state doublet [7, 8]. When combined with an AIAO ground state, the symmetry properties of this dipolar-octupolar doublet allow the decoupling of the divergence-full (AIAO) and divergence-free (spin ice) fluctuations [12]. Here we use neutron spectroscopy to determine the dipolar-octupolar nature of the crystal field ground state doublet of $Sm_2Ti_2O_7$ and use neutron diffraction to show that it orders into an AIAO structure below $T_N = 0.35$ K. Muon spin relaxation measurements reveal persistent spin dynamics within the magnetically ordered state, down to 0.03 K. Thus, we demonstrate that $Sm_2Ti_2O_7$ possesses the requisite ingredients for moment fragmentation physics.

In contrast to the extensive studies that have been performed on the other magnetic titanate pyrochlores, $R_2Ti_2O_7$ (R = Gd, Tb, Dy, Ho, Er, Yb), the magnetic properties of $Sm_2Ti_2O_7$ have remained largely unexplored. Prior studies of $Sm_2Ti_2O_7$ were limited to bulk property measurements in the paramagnetic regime, above 0.5 K, which revealed weak antiferromagnetic interactions ($\theta_{CW} = -0.26$ K) [13]. While the other above-mentioned titanate pyrochlores have been the subjects of a plethora of elastic and inelastic neutron scattering experiments, equivalent experiments on $Sm_2Ti_2O_7$ are daunting. The first reason is the size of the Sm^{3+} magnetic moment; the Lande g-factor associated with the $4f^5$ electronic configuration is its smallest possible non-zero value ($g_J = {}^2\!/_7$), giving rise to small moments even in the absence of crystal field effects (which make the moment smaller still). This small magnetic moment represents a significant hindrance because scattered neutron intensity varies as the moment squared. Compounding this effect is that naturally-occurring samarium is a very strong neutron absorber due to the presence of ^{149}Sm at the 13.9% level ($\sigma_{abs} = 42,000$ barns). Neutron scattering measurements of the type we report here are only possible with a sample isotopically-enriched with ^{154}Sm ($\sigma_{abs} = 8.4$ barns). However, the neutron absorption cross section of ^{149}Sm is so high that even trace amounts result in a sample that is still strongly absorbing by neutron scattering standards.

We grew a large single crystal of $Sm_2Ti_2O_7$ with the optical floating zone technique using 99.8% enriched $^{154}Sm_2O_3$ (Cambridge Isotopes). Low-temperature heat capacity measurements were performed using the quasi-adiabatic technique. Neutron diffraction measurements were performed on the D7 polarized diffuse scattering spectrometer at the Institute Laue-Langevin and beam line HB-1A at the High Flux Isotope Reactor at Oak Ridge National Laboratory (ORNL). Inelastic neutron scattering measurements were performed on the ARCS [14] and SEQUOIA [15] spectrometers at the Spallation Neutron Source at ORNL. Muon spin relaxation measurements were carried out at TRIUMF. Further experimental details are provided in the Supplementary Materials [16].

The Hund's rules ground state for Sm^{3+} is $J = {}^5\!/_2$. Accordingly, in the reduced symmetry environment of the pyrochlore lattice, the $2J + 1 = 6$ states split into three Kramers' doublets, one of which forms the crystal electric field (CEF) ground state. Inelastic neutron scattering (INS) measurements on $Sm_2Ti_2O_7$, which are presented in Fig. 1 and Fig. S2, show intense excitations at 16.3(5) and 70.0(5) meV corresponding to transitions to the excited CEF doublets. The lower energy excitation is consistent with one of the modes previously identified in Raman scattering experiments by Singh *et al* [13]. However, other modes observed in Raman scattering and originally attributed to additional CEF excitations are not visible in our INS data. Malkin *et al.* attempted to determine the crystal field parameters of $Sm_2Ti_2O_7$ by modeling magnetic susceptibility data [17]. This work predicts CEF levels at 21.4 and 26.4 meV, both of which are inconsistent with our INS data. It is worth noting that Sm^{3+} has a rather atypical form factor, which rather than monotonically decreasing with Q instead reaches its maximum value near 5 Å^{-1}. Both of the CEF transitions

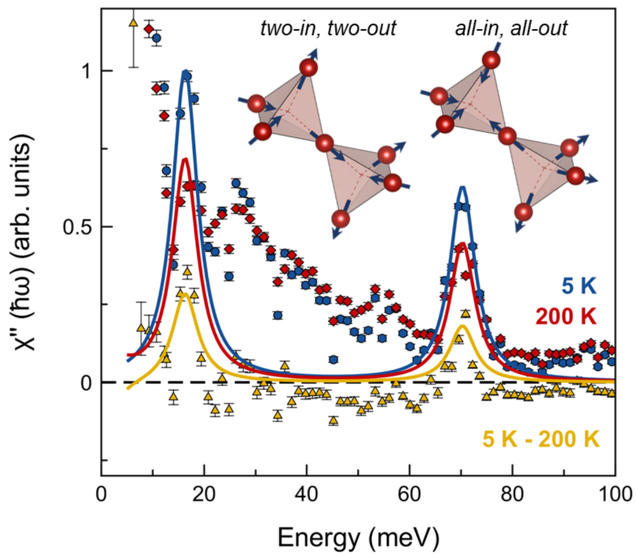

FIG. 1. Inelastic neutron scattering measurements of the crystal electric field (CEF) excitations in $Sm_2Ti_2O_7$ at 5 K (red) and 200 K (blue). The temperature difference (yellow) confirms the presence of two CEF levels, at 16.3(5) meV and 70.0(5) meV. The fits to the data with our CEF model are given by the solid lines and reveal the Ising nature of the Sm^{3+} moments in $Sm_2Ti_2O_7$. The insets show the ferromagnetic Ising spin configuration (two-in, two-out) and the antiferromagnetic Ising spin configuration (all-in, all-out).

TABLE I. Result of the CEF analysis for $Sm_2Ti_2O_7$, calculated within a point charge model and then refined by fitting the two experimentally observed CEF excitations.

E_{obs} (meV)	E_{fit} (meV)	$\lvert \pm {}^5\!/_2 \rangle$	$\lvert \pm {}^3\!/_2 \rangle$	$\lvert \pm {}^1\!/_2 \rangle$
0.0	0.0	0	1	0
16.3(5)	16.5	0	0	1
70.0(5)	70.3	1	0	0

observed here obey this form factor (see Supplmentary Materials [16]). These two excitated states account for the full manifold associated with the $J = 5/2$ ground state multiplet.

Next, we modeled the INS data in order to extract the crystal field Hamiltonian. This analysis is complicated by the strong residual absorption of ^{149}Sm in the isotopically-enriched single crystal. This issue was addressed by performing an absorption correction with Monte Carlo ray tracing simulations using MCViNE [18]. In the case of Sm^{3+}, the Hund's rules J manifold is separated from the first excited spin-orbit manifold by $\lambda(J+1) \approx 500$ meV [19]. Incorporating this higher manifold into our analysis would require the introduction of four additional free parameters. This would result in an under constrained parameterization of the CEF Hamiltonian and thus, we have neglected it here. Further details of these calculations and the subsequent determination of the CEF eigenvalues and eigenvectors are presented in the Supplementary Material [16].

The CEF parameters that provide the best fit to our INS data for $Sm_2Ti_2O_7$ within a point charge approximation are: $B_{20} = 3.397$ meV, $B_{40} = 0.123$ meV, and $B_{43} = 8.28 \cdot 10^{-8}$ meV. Table I shows the resulting CEF eigenvectors and eigenvalues. Our refinement gives a ground-state doublet of pure $|m_J = \pm 3/2\rangle$ character. The three-fold rotational symmetry at the rare earth site implies that states within a time-reversal symmetry-paired Kramers doublet must be composed of m_J basis states separated by three units. Accordingly, in our case where the maximum $m_J = 5/2$, it follows that the doublet composed of $|m_J = \pm 3/2\rangle$ cannot be coupled to any other basis state and is hence, necessarily pure. The symmetry nature of this doublet imparts it with an exotic character: while two components of the pseudospin transform like a magnetic dipole, the third component transforms as a component of the magnetic octupole tensor [20]. Thus, the ground state doublet in $Sm_2Ti_2O_7$ is termed a dipolar-octupolar doublet. This result distinguishes $Sm_2Ti_2O_7$ from other antiferromagnetic Kramers $R_2Ti_2O_7$ pyrochlores (R = Er [21] and Yb [22]), which possess ground state doublets that transform simply as a magnetic dipole, effectively mimicking a true $S = 1/2$. Our refined g-tensor gives $g_z = 0.857(9)$ and $g_{xy} = 0.0$, corresponding to Ising anisotropy, where the spins point along their local [111] direction, which connects the vertices of the tetrahedron to its center (inset of Fig. 1). The magnetic moment within the ground state doublet of Sm^{3+} is $\mu_{\mathrm{CEF}} = 0.43(6)\ \mu_B$.

Finally, as originally discussed in Ref. [23], we can take advantage of the fact that extensive CEF studies have been performed on other rare earth titanate pyrochlores [21, 22, 24–27], allowing us to use scaling arguments. An especially good starting point is Er^{3+} in $Er_2Ti_2O_7$, which has a large total angular momentum, $J = 15/2$. This material has seven excited crystal field levels, all of

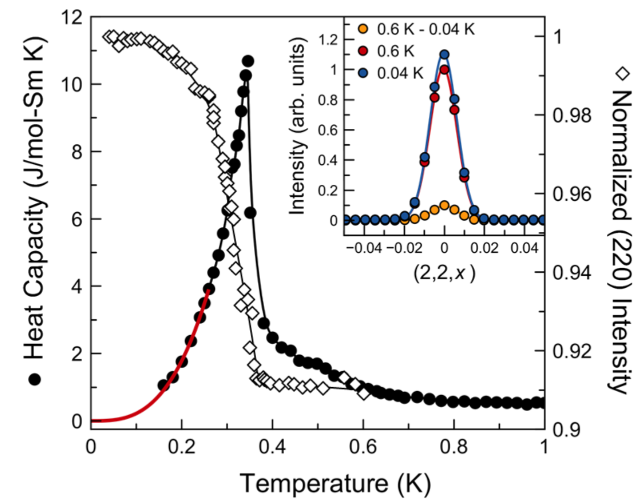

FIG. 2. $Sm_2Ti_2O_7$ undergoes a long-range magnetic ordering transition at $T_N = 0.35$ K. The black circles represent the heat capacity, which shows a sharp anomaly at T_N and a T^3 dependence at the lowest temperatures, as indicated by the red line. The open diamonds represent the intensity of the (220) Bragg peak, which shows an abrupt increase at T_N. The black lines are guides to the eye. The inset shows a scan over the (220) Bragg peak above and below T_N, where the enhanced intensity corresponds to the formation of a magnetic Bragg peak.

which were observed in a recent INS study, leading to a highly constrained CEF Hamiltonian [21]. Armed with these results, scaling arguments give us qualitatively good agreement with the known CEF manifolds for $R_2Ti_2O_7$ (R = Ho, Tb, and Yb) [21]. When applied to $Sm_2Ti_2O_7$, these same scaling arguments predict the CEF ground state to be pure $|m_J = \pm 3/2\rangle$ with a large energy gap to the first excited state, consistent with our experimental determination.

We next turn to the low-temperature collective magnetic properties of $Sm_2Ti_2O_7$. The heat capacity of $Sm_2Ti_2O_7$, shown in Fig. 2(a), contains a lambda-like anomaly at $T_N = 0.35$ K, indicative of a second-order phase transition to a long-range magnetically ordered state. This ordering transition was not observed in previous studies as their characterization measurements did not extend below 0.5 K [13]. The low temperature region of the anomaly, below 0.3 K, is well-fit by a T^3 power law, consistent with gapless, three-dimensional antiferromagnetic spin waves. In order to compute the entropy release associated with this anomaly, we extrapolate the T^3 behavior to 0 K. Then, an integration of C/T up to 1 K returns an entropy of $0.84 \cdot R \ln 2$, close to the full $R \ln 2$ expected for a well-isolated Kramers doublet. Thus, a small fraction of the entropy release in this system may be taking place at temperatures above 1 K or some fraction of the moment may remain dynamic below T_N.

We used the D7 polarized neutron scattering spectrometer at the ILL to search for magnetic diffuse scattering

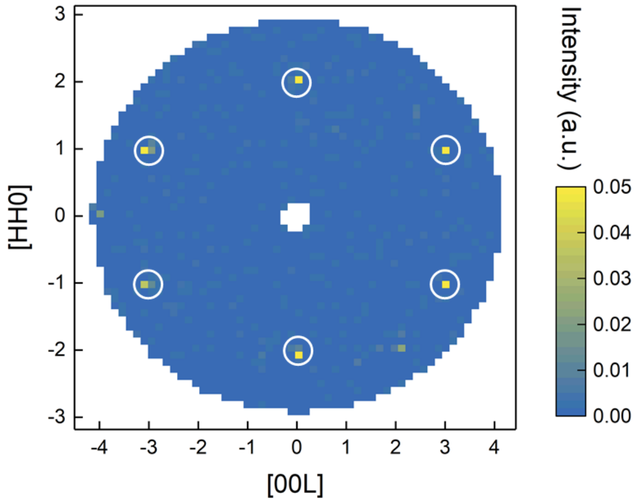

FIG. 3. Spin flip channel of polarized neutron scattering measurements on $Sm_2Ti_2O_7$ in the (HHL) scattering plane at 0.05 K. Magnetic Bragg peaks are observed to form on the (220) and (113) positions and are absent at the (111), (002), (222) and (004) positions. Symmetry analysis of this magnetic diffraction pattern reveals that $Sm_2Ti_2O_7$ is ordering into the Γ_3 AIAO state with an ordered moment of $\mu_{ord} = 0.44(7)\ \mu_B$. Note that weak bleed-through of nuclear Bragg intensity has been corrected by subtracting a high temperature (4 K) data set.

in $Sm_2Ti_2O_7$. While none could be resolved above or below T_N, we did observe the formation of magnetic Bragg peaks at the (220) and (113) positions in the spin flip channel (Figure 3). The observed magnetic Bragg reflections were indexed against the possible $\vec{k} = 0$ ordered structures for the 16c Wyckoff position in the $Fd\bar{3}m$ pyrochlore lattice (Table II). The errors on the observed peak intensities are rather high due to the small magnetic signals ($\mu_{\rm ord} \leq \mu_{\rm CEF} = 0.43\ \mu_B$) located on large nuclear Bragg peaks, the absorption from residual ^{149}Sm, as well as the relatively poor Q-resolution of a diffuse scattering instrument. However, as can be seen by careful examination of Table II, the observed magnetic Bragg reflections nicely map onto the Γ_3 irreducible representation. All other representations can be ruled out by the absence of magnetic reflections at the (002) and (111) positions in the experimental data. Γ_3 corresponds to the AIAO magnetic structure (right inset of Fig 1), which is the expected result when Ising anisotropy is combined with net antiferromagnetic exchange interactions. The neutron order parameter, shown in Fig. 2, reveals a sharp onset below $T_N = 0.35$ K, fully-consistent with the anomaly observed in the heat capacity.

While the D7 data allowed a definitive determination of the magnetic structure of $Sm_2Ti_2O_7$, it is not appropriate for estimating the value of the ordered moment due to the coarse Q-resolution of the instrument. The triple axis spectrometer HB-1A, with its significantly-improved Q-resolution, was therefore used for this purpose. Since HB-1A uses an unpolarized neutron beam, magnetic intensity was only observed at the (220) Bragg peak position in this experiment, which corresponds to the strongest magnetic reflection expected for the AIAO magnetic structure but also a relatively weak nuclear Bragg peak. We determined the Sm^{3+} ordered magnetic moment by comparing the ratio of the magnetic intensity to the nuclear intensity at this Bragg position. This procedure, which incorporated both the j_0 and j_2 spherical Bessel function contributions to the Sm^{3+} magnetic form factor, yielded an ordered moment of $\mu_{\rm ord} = 0.44(7)\ \mu_B$.

TABLE II. Bragg peak intensities for the possible $\vec{k} = 0$ magnetic structures for $Sm_2Ti_2O_7$. The best agreement is obtained with the Γ_3 all-in all-out structure.

	(111)	(002)	(222)	(220)	(113)	(004)
Observed	0	0	0	1.0±0.4	0.78±0.27	0
Γ_3	0	0	0	1.00	0.66	0
Γ_5	0.88	0	0	1	0.35	0
Γ_7	0.52	1.00	0.44	0.11	0	0
Γ_9 [110]	0.69	1.00	0.44	0.43	0.51	0.67
Γ_9 [100]	0.06	0.37	0.16	0.44	0.76	1.00

Last, we turn to zero-field muon spin relaxation (μSR) measurements on $Sm_2Ti_2O_7$, the results of which are presented in Fig. 4. The temperature-independent contribution from muons that land outside the sample has been subtracted, leaving only the sample asymmetry. At 1 K and above, the asymmetry is non-relaxing, indicating that the Sm^{3+} moments are in a fast-fluctuating paramagnetic regime. Approaching T_N, the relaxation gradually increases, consistent with a critical slowing of the spin dynamics. Over the full temperature range, the asymmetry is well-described by a Gaussian relaxation, $A(t) = A_0 e^{-\lambda t^2}$, where λ is the temperature-dependent relaxation rate. The fitted relaxation rates, which are weak at all temperatures, are plotted in the inset of Fig. 4 where we see the rate sharply increase at T_N and then ultimately plateaus below 0.2 K.

In a small moment sample such as $Sm_2Ti_2O_7$, where the background relaxation is weak, one would expect to observe spontaneous oscillations in the asymmetry spectra below T_N. However, they are strikingly absent in our measurement. The Gaussian relaxation observed here, combined with the lack of oscillations in the asymmetry spectra below T_N, is reminiscent of recent μSR measurements on another Ising antiferromagnet, $Nd_2Zr_2O_7$ [28]. In that case, the Gaussian relaxation was attributed to strong spin fluctuations that coexist microscopically with AIAO magnetic order, which generates a dynamic local magnetic field at the muon sites below T_N. This coexistance is argued to arise from magnetic moment fragmentation, which had been demonstrated in $Nd_2Zr_2O_7$ via neutron scattering [8, 10]. More specifically, the INS

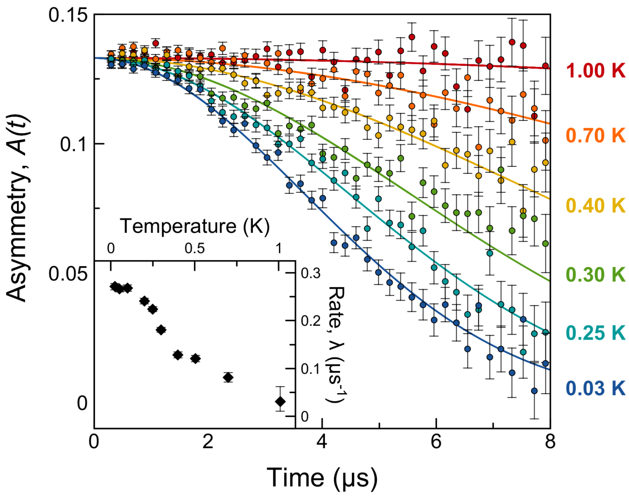

FIG. 4. The μSR asymmetry spectra of $Sm_2Ti_2O_7$ between 1.00 K and 0.03 K, which are well-fit by a Gaussian relaxation, indicated by the solid lines. The temperature dependence of the relaxation rate, λ, extracted from these fits is shown in the inset. Below T_N, λ is observed to plateau indicative of persistent spin dynamics in the ordered state. The absence of an oscillatory component in the asymmetry is consistent with moment fragmentation.

data on $Nd_2Zr_2O_7$ revealed that the dynamic component of the ground state has a characteristic frequency on the order of 10^{10} Hz which is well within the μSR timescale. The persistent spin dynamics observed in our μSR spectra for $Sm_2Ti_2O_7$ could well arise from a similar origin. The absence of oscillations in an ordered state may also arise from a cancellation of the static dipolar field at the muon site from different ordered moments. However, this scenario is ruled out here by three simple observations: (1) there are no potential high-symmetry muon sites in the pyrochlore structure where the field could cancel by symmetry, (2) an oscillatory component *has been* observed in the μSR of another AIAO pyrochlore $Nd_2Sn_2O_7$ [6], where it is important to note that, unlike $Nd_2Zr_2O_7$, fragmentation physics has not been demonstrated and (3) $Sm_2Ti_2O_7$ is iso-structural with $Nd_2Sn_2O_7$ and therefore the muon stopping sites are expected to be very similar.

We have demonstrated that $Sm_2Ti_2O_7$ possesses all the requisite ingredients for moment fragmentation physics. Crystal field analysis of our neutron spectroscopy measurements confirms that $Sm_2Ti_2O_7$ has an Ising dipolar-octupolar crystal field ground state doublet. Through symmetry analysis of our neutron diffraction data, we find that $Sm_2Ti_2O_7$ orders into an all-in, all-out magnetic structure below $T_N = 0.35$ K, with an ordered moment of $\mu_{\rm ord} = 0.44(7)\ \mu_B$. Muon spin relaxation measurements identify persistent spin dynamics to temperatures well-below T_N and an absence of oscillations, consistent with a fragmentation scenario.

This research was supported by NSERC of Canada. A portion of this research used resources at the High Flux Isotope Reactor and Spallation Neutron Source, a DOE Office of Science User Facility operated by the Oak Ridge National Laboratory. CRW thanks the Canada Research Chair program (Tier II). CM thanks the Manitoba Government for support through the MGS. JAQ acknowledges technical support from M. Lacerte and S. Fortier and funding from FRQNT and CFREF. GS thanks J. Lin and A.T. Savici for useful discussions, and support in the analysis. HDZ acknowledges support from NSF DMR through Grant No. DMR-1350002.

[1] Jason S Gardner, Michel JP Gingras, and John E Greedan, "Magnetic pyrochlore oxides," Reviews of Modern Physics **82**, 53 (2010).
[2] MJ Harris, ST Bramwell, DF McMorrow, Th Zeiske, and KW Godfrey, "Geometrical frustration in the ferromagnetic pyrochlore $Ho_2Ti_2O_7$," Physical Review Letters **79**, 2554 (1997).
[3] Arthur P Ramirez, A Hayashi, RJ Cava, R Siddharthan, and BS Shastry, "Zero-point entropy in spin ice," Nature **399**, 333 (1999).
[4] Steven T Bramwell and Michel JP Gingras, "Spin ice state in frustrated magnetic pyrochlore materials," Science **294**, 1495–1501 (2001).
[5] Byron C den Hertog and Michel JP Gingras, "Dipolar interactions and origin of spin ice in Ising pyrochlore magnets," Physical Review Letters **84**, 3430 (2000).
[6] Alexandre Bertin, P Dalmas de Réotier, B Fåk, Christophe Marin, Alain Yaouanc, A Forget, D Sheptyakov, Bernhard Frick, C Ritter, A Amato, *et al.*, "$Nd_2Sn_2O_7$: An all-in–all-out pyrochlore magnet with no divergence-free field and anomalously slow paramagnetic spin dynamics," Physical Review B **92**, 144423 (2015).
[7] J Xu, VK Anand, AK Bera, M Frontzek, Douglas L Abernathy, N Casati, K Siemensmeyer, and B Lake, "Magnetic structure and crystal-field states of the pyrochlore antiferromagnet $Nd_2Zr_2O_7$," Physical Review B **92**, 224430 (2015).
[8] Elsa Lhotel, Sylvain Petit, Solène Guitteny, O Florea, M Ciomaga Hatnean, Claire Colin, Eric Ressouche, MR Lees, and G Balakrishnan, "Fluctuations and all-in–all-out ordering in dipole-octupole $Nd_2Zr_2O_7$," Physical Review Letters **115**, 197202 (2015).
[9] VK Anand, AK Bera, J Xu, T Herrmannsdörfer, C Ritter, and B Lake, "Observation of long-range magnetic ordering in pyrohafnate $Nd_2Hf_2O_7$: a neutron diffraction study," Physical Review B **92**, 184418 (2015).
[10] Sylvain Petit, Elsa Lhotel, Benjamin Canals, M Ciomaga Hatnean, Jacques Ollivier, Hannu Mutka, Eric Ressouche, AR Wildes, MR Lees, and G Balakrishnan, "Observation of magnetic fragmentation in spin ice," Nature Physics **12**, 746 (2016).
[11] ME Brooks-Bartlett, Simon T Banks, Ludovic DC Jaubert, Adam Harman-Clarke, and Peter CW Holdsworth, "Magnetic-moment fragmentation and monopole crystallization," Physical Review X **4**, 011007 (2014).
[12] Owen Benton, "Quantum origins of moment fragmenta-

tion in $Nd_2Zr_2O_7$," Physical Review B **94**, 104430 (2016).
[13] Surjeet Singh, Surajit Saha, SK Dhar, R Suryanarayanan, AK Sood, and A Revcolevschi, "Manifestation of geometric frustration on magnetic and thermodynamic properties of the pyrochlores $Sm_2X_2O_7$ (X = Ti, Zr)," Physical Review B **77**, 054408 (2008).
[14] Douglas L Abernathy, Matthew B Stone, MJ Loguillo, MS Lucas, O Delaire, Xiaoli Tang, JYY Lin, and B Fultz, "Design and operation of the wide angular-range chopper spectrometer ARCS at the Spallation Neutron Source," Review of Scientific Instruments **83**, 015114 (2012).
[15] GE Granroth, AI Kolesnikov, TE Sherline, JP Clancy, KA Ross, JPC Ruff, BD Gaulin, and SE Nagler, "SEQUOIA: a newly operating chopper spectrometer at the SNS," in *Journal of Physics: Conference Series*, Vol. 251 (IOP Publishing, 2010) p. 012058.
[16] See Supplementary Material [url] for further information on the crystal growth, experimental details, and the crystal field analysis. Works cited in the Supplementary Material are Refs. [18, 21, 23, 29–35].
[17] BZ Malkin, TTA Lummen, PHM Van Loosdrecht, G Dhalenne, and AR Zakirov, "Static magnetic susceptibility, crystal field and exchange interactions in rare earth titanate pyrochlores," Journal of Physics: Condensed Matter **22**, 276003 (2010).
[18] Jiao YY Lin, Hillary L Smith, Garrett E Granroth, Douglas L Abernathy, Mark D Lumsden, Barry Winn, Adam A Aczel, Michael Aivazis, and Brent Fultz, "MCViNE–an object oriented monte carlo neutron ray tracing simulation package," Nucl. Instr. Meth. Phys. Res. **810**, 86–99 (2016).
[19] M Blume, AJ Freeman, and RE Watson, "Theory of spin-orbit coupling in atoms. III," Physical Review **134**, A320 (1964).
[20] Yi-Ping Huang, Gang Chen, and Michael Hermele, "Quantum spin ices and topological phases from dipolar-octupolar doublets on the pyrochlore lattice," Physical Review Letters **112**, 167203 (2014).
[21] J Gaudet, AM Hallas, AI Kolesnikov, and BD Gaulin, "Effect of chemical pressure on the crystal electric field states of erbium pyrochlore magnets," Physical Review B **97**, 024415 (2018).
[22] J Gaudet, DD Maharaj, G Sala, E Kermarrec, KA Ross, HA Dabkowska, AI Kolesnikov, GE Granroth, and BD Gaulin, "Neutron spectroscopic study of crystalline electric field excitations in stoichiometric and lightly stuffed $Yb_2Ti_2O_7$," Physical Review B **92**, 134420 (2015).
[23] M.T. Hutchings, "Point-charge calculations of energy levels of magnetic ions in crystalline electric fields," (Academic Press, 1964) pp. 227 – 273.
[24] S Rosenkranz, AP Ramirez, A Hayashi, RJ Cava, R Siddharthan, and BS Shastry, "Crystal-field interaction in the pyrochlore magnet $Ho_2Ti_2O_7$," Journal of Applied Physics **87**, 5914–5916 (2000).
[25] A Bertin, Y Chapuis, P Dalmas de Réotier, and A Yaouanc, "Crystal electric field in the $R_2Ti_2O_7$ pyrochlore compounds," Journal of Physics: Condensed Matter **24**, 256003 (2012).
[26] M Ruminy, E Pomjakushina, K Iida, K Kamazawa, DT Adroja, U Stuhr, and T Fennell, "Crystal-field parameters of the rare-earth pyrochlores $R_2Ti_2O_7$ (R = Tb, Dy, and Ho)," Physical Review B **94**, 024430 (2016).
[27] AJ Princep, HC Walker, DT Adroja, D Prabhakaran, and AT Boothroyd, "Crystal field states of Tb^{3+} in the pyrochlore spin liquid $Tb_2Ti_2O_7$ from neutron spectroscopy," Physical Review B **91**, 224430 (2015).
[28] J Xu, C Balz, C Baines, H Luetkens, and B Lake, "Spin dynamics of the ordered dipolar-octupolar pseudospin-1/2 pyrochlore $Nd_2Zr_2O_7$ probed by muon spin relaxation," Physical Review B **94**, 064425 (2016).
[29] AS Wills, "A new protocol for the determination of magnetic structures using simulated annealing and representational analysis (SARAh)," Physica B: Condensed Matter **276**, 680–681 (2000).
[30] Juan Rodríguez-Carvajal, "Recent advances in magnetic structure determination by neutron powder diffraction," Physica B: Condensed Matter **192**, 55–69 (1993).
[31] M Ruminy, M Núñez Valdez, Björn Wehinger, A Bosak, DT Adroja, U Stuhr, K Iida, K Kamazawa, E Pomjakushina, D Prabakharan, *et al.*, "First-principles calculation and experimental investigation of lattice dynamics in the rare-earth pyrochlores $R_2Ti_2O_7$ (R = Tb, Dy, Ho)," Physical Review B **93**, 214308 (2016).
[32] KWH Stevens, "Matrix elements and operator equivalents connected with the magnetic properties of rare earth ions," Proceedings of the Physical Society. Section A **65**, 209 (1952).
[33] U Walter, "Treating crystal field parameters in lower than cubic symmetries," Journal of Physics and Chemistry of Solids **45**, 401–408 (1984).
[34] John L Prather, *Atomic energy levels in crystals*, Tech. Rep. (National Bureau of Standards, Gaithersburg MD, 1961).
[35] Osvald Knop, François Brisse, and Lotte Castelliz, "Pyrochlores V: Thermoanalytic, x-ray, neutron, infrared, and dielectric studies of $A_2Ti_2O_7$ titanates," Canadian Journal of Chemistry **47**, 971–990 (1969).